

Lethal and nonlethal murine malarial infections differentially affect apoptosis, proliferation, and CD8 expression on thymic T cells

S. KHANAM,[†] S. SHARMA & S. PATHAK

Department of Biological Sciences, Tata Institute of Fundamental Research, Mumbai, Maharashtra, India

SUMMARY

Although thymic atrophy and apoptosis of the double-positive (DP) T cells have been reported in murine malaria, comparative studies investigating the effect of lethal and nonlethal *Plasmodium* infections on the thymus are lacking. We assessed the effects of *P. yoelii* lethal (17XL) and nonlethal (17XNL) infections on thymic T cells. Both strains affected the thymus. 17XL infection induced DP T-cell apoptosis and a selective decrease in surface CD8 expression on developing thymocytes. By contrast, more severe but reversible effects were observed during 17XNL infection. DP T cells underwent apoptosis, and proliferation of both DN and DP cells was affected around peak parasitemia. A transient increase in surface CD8 expression on thymic T cells was also observed. Adult thymic organ culture revealed that soluble serum factors, but not IFN- γ or TNF- α , contributed to the observed effects. Thus, lethal and nonlethal malarial infections led to multiple disparate effects on thymus. These parasite-induced thymic changes are expected to impact the naïve T-cell repertoire and the subsequent control of the immune response against the parasite. Further investigations are required to elucidate the mechanism responsible for these disparate effects, especially the reversible involution of the thymus in case of nonlethal infection.

Keywords 17XL, 17XNL, apoptosis, *Plasmodium yoelii*, T-cell development, thymic atrophy

Correspondence: Sulabha Pathak, B332, Department of Biological Sciences, Tata Institute of Fundamental Research, 1, Homi Bhabha Road, Colaba, Mumbai 400005, India (e-mail: pathaksue@gmail.com).

[†]Present address: Cactus Communications Pvt. Ltd., 511 Shalimar Morya Park, Off Link Road, Andheri West, Mumbai 400 053, India

Disclosures: The authors have no conflict of interests to declare.

Received: 1 July 2014

Accepted for publication: 11 April 2015

BACKGROUND

Malaria, a devastating illness caused by bloodborne protozoan parasites belonging to *Plasmodium* spp, may remain uncomplicated or may result in severe disease leading to lethality. Studies on murine malaria models have led to a better understanding of the pathogenesis of the disease and the immune responses it elicits (1,2). Four species of the malarial parasite, *P. chabaudi*, *P. vinckei*, *P. berghei* and *P. yoelii*, are used in experimental infections, and they vary in their pathogenicity and the immune response they induce (3,4). There are reports that demonstrate a reduction in thymic cellularity post-infection using some of these *Plasmodium* species (5–7); however, till date, there are no systematic studies investigating the effect of lethal and nonlethal malarial infections on the murine thymus. A comparative evaluation of a severe vs. self-limiting malarial infection will further our understanding of the malaria-induced effects on the thymus. *P. yoelii* is well suited to study such immunological aspects of the infection (1). The two strains of this parasite, 17XL (lethal) and 17XNL (nonlethal), differ in their growth kinetics, cellular tropisms, the type of immune responses they invoke and the clinical outcomes of their infections (8–10). The virulent 17XL strain infects mainly mature erythrocytes, whereas the 17XNL strain preferentially infects reticulocytes (8). This preference for a particular erythrocyte type has been traced to single Cys to Arg replacement in the erythrocyte binding-like protein involved in parasite invasion (9). Two other markers that are not linked to the erythrocyte binding-like protein are also thought to play a role in the virulence of these strains (10). However, such specificity defines the cell selection for invasion and does not reflect on the subsequent molecular events leading to the virulent vs. nonvirulent phenotypes. The two strains induce distinct peripheral immune responses, especially in terms of the nature and kinetics of IFN- γ and TGF- β induction (11–13). The two infections have also been shown to differ in their effect on

the spleen (11). 17XNL infection causes a temporary closure of spleen circulation with the formation of syncytial layers of fibroblasts that form physical barriers (14); such remodelling does not occur in 17XL infection.

Thymic T-cell development occurs in discrete stages comprising differentiation, proliferation, selective apoptosis and egress that finally results in a T-cell repertoire capable of providing protection against invaders while being tolerant to self-antigens. The process starts with thymic progenitor cells from the bone marrow entering the thymic cortex (15,16). These progenitors express neither CD4 nor CD8 and are termed 'double negative (DN)'. The DN stage consists of four substages (DN1–DN4) defined by the expression of CD25 and CD44. As they migrate through the thymus, the DN cells rearrange their T-cell receptor (TcR) genes and first start expressing CD8 to become immature single-positive cells and then CD4 to become CD4⁺CD8⁺ double-positive (DP) T cells. The developing thymocytes undergo extensive antigen-independent proliferation at two discrete steps during their transition from the DN to the DP stage to provide sufficient numbers of thymocytes for the ensuing stringent selection processes (17,18). Subsequent positive and negative selection ensures that the cells that do not express TcRs recognizing self-MHC molecules and those that express TcRs with high affinity for self-MHC molecules or self-antigens undergo apoptosis. Almost 95% of all thymocytes die in the thymus because of these selection processes (19–21). DP T cells that survive the selection processes lose one of the markers to become either CD4 or CD8 single-positive (SP) T cells and eventually egress the thymus to replenish the peripheral naïve T-cell compartment. Although the thymus involutes with age, it continues to produce naïve T cells. This comparative study investigates the effects of 17XL and 17XNL infections on the host thymus. We show that both strains result in an atrophy of the thymus and affect apoptosis and proliferation of developing T-cell subpopulations. DP T cells were predominantly affected in 17XL infection, whereas DN, DP, and CD4⁺ SP T-cell subpopulations underwent drastic reduction in numbers during the ascending phase of 17XNL infection. *P. yoelii* 17XL infection resulted in decreased surface CD8 expression on developing thymocytes at the peak of parasitemia. However, 17XNL infection did not affect CD8 surface expression except an upward trend during the early phase of infection. Adult thymic organ culture (ATOC) revealed that these effects in case of 17XL infection were not attributable to either IFN- γ or TNF- α . Thus, the two strains distinctly affected thymic T-cell numbers, apoptosis and proliferation. In summary, more severe effects were observed during 17XNL infection at a much lower parasit-

emia (%parasitemia = 5.52 ± 1.41) when compared to 17XL infection (%parasitemia = 53.93 ± 18.86).

MATERIALS AND METHODS

Mice

Male BALB/*c* mice (6–8 weeks old) were obtained from the local animal breeding facility at the Tata Institute of Fundamental Research, Mumbai, India. Mice were bred and maintained under specific pathogen-free conditions. All experiments were conducted in accordance with the guidelines and recommendations of the Committee for the Purpose of Control and Supervision on Experiments on Animals, Tata Institute of Fundamental Research.

Parasites and infection

P. yoelii 17XL and 17XNL strains were revived from frozen stocks. The infection was initiated by intraperitoneal (i.p.) injection of 10^4 parasitized RBCs (1). Progress of infection was monitored by microscopic examination of Giemsa-stained thin blood smears. All experiments were carried out at least thrice, and three mice were sacrificed at each time point tested. The data for each time point are represented as mean \pm SEM ($n = 3$).

Antibodies and other reagents

The following antibodies and reagents were obtained from BD Pharmingen (San Diego, CA, USA): PE-labelled anti-mouse CD4 (#553652), PE-Cy5-labelled anti-mouse CD8 (#553034), FITC-labelled anti-mouse Thy 1.2 (#553013), FITC-labelled anti-BrdU (#556028), FITC-labelled Annexin V (#556419), purified anti-mouse CD16/32 (#553142), peroxidase-labelled goat anti-mouse IgG (#554002), anti-mouse IFN- γ -neutralizing antibody (#551216) and propidium iodide staining solution (#556463). Anti-mouse TNF- α -neutralizing antibody (#506105) was purchased from BioLegend Inc, San Diego, CA, USA. Protein G-sepharose beads were obtained from GE Healthcare Life Sciences, Buckinghamshire, UK.

Flow cytometry

Cell surface staining

Thymi and spleens were harvested, single-cell suspensions were prepared, and erythrocytes were removed by lysis using ACK buffer (0.15 M NH₄Cl, 10 mM KHCO₃, 0.1 mM Na₂EDTA). The cells were resuspended in FACS buffer (1% v/v FBS and 0.01% NaN₃ in PBS) and incubated with blocking antibody (anti-mouse CD16/32) for 15 min at RT

(room temperature) prior to incubation with respective antibodies and isotype controls for 20 min at 4°C (5).

Apoptosis detection

Thymocytes were resuspended in 100 µL annexin-binding buffer (10 mM HEPES, 140 mM NaCl and 2.5 mM CaCl₂, pH 7.4) followed by staining with FITC-labelled annexin V, anti-CD4 and anti-CD8 antibodies for 15 min at RT according to manufacturer's instructions (Sigma-Aldrich, St. Louis, MO, USA). Alternatively, 1 million cells were incubated on ice with 10 µL of PI solution (50 µg/mL) for 10 min followed by acquisition on a flow cytometer.

BrdU labelling and detection

One milligram Bromodeoxyuridine (Roche, Basel, Switzerland) dissolved in 0.15 M NaCl was administered as a single i.p. injection. The mice were sacrificed 2 h post-injection. The thymocytes were processed for detection of BrdU incorporation as described by Lucas *et al.* (22). Briefly, the cells were resuspended in ice-cold 0.15 M NaCl, fixed with 95% ethanol at -20°C, permeabilized using 1% paraformaldehyde and 0.01% Tween-20 in PBS for 30 min at 4°C, and incubated with DNase I buffer (0.15 M NaCl, 4.2 mM MgCl₂, 10 µM HCl and 50 000 units/mL DNase I) for 40 min at 37°C. The cells were then stained with FITC-labelled anti-BrdU antibody for 30 min at RT.

All samples were acquired on PAS, Partec (Gorlitz, Germany), and analysed using FLOMAX software (Partec, Gorlitz, Germany).

H & E staining

The sectioning and staining of the thymi were carried out as described by Achtman *et al.* (23). Thymi were snap-frozen in liquid nitrogen, embedded in cold OCT compound, and serial 5-µm cryosections were mounted on glass slides. Slides were allowed to dry at RT followed by fixation in 90% acetone at 4°C for 20 min. The sections were stained with haematoxylin (Sigma-Aldrich) and eosin (Sigma-Aldrich) as per manufacturer's instructions. Briefly, the slides were first stained in haematoxylin solution for 1.5–3 min, washed and incubated for 20–60 s in acid alcohol. After washing, the slides were incubated in Scott's Tap Water Substitute for 5–60 s, counterstained with eosin, dehydrated in graded alcohol, cleared with Histoclear (Fisher Scientific, Waltham, MA, USA) and mounted in DPX (Sigma-Aldrich). The slides were observed under Olympus BX41 microscope (20× magnification), and images were captured using Nikon D50 camera.

Adult Thymic Organ Culture

Thymic explant culture was carried out as described by Whalen *et al.* (24). 1-mm³ thymic explants were cut using

McIlwan tissue chopper and cultured on filters (0.45-µm filters, Millipore, Bedford, MA, USA) placed on top of Ab-gel gelatin sponges (Shri Gopal Krishna Laboratories, Mumbai, India) placed in 6-well plates. The sponges were hydrated overnight in DMEM at 37°C and 5% CO₂ atmosphere prior culture. The thymic explants were cultured at 37°C and 5% CO₂ atmosphere in DMEM + 10% normal mouse serum and supplemented with various factors (outlined below) for 12 or 24 h as indicated. The cells were extracted from explants by homogenization and assessed for viability, CD4, and CD8 expression as described. The culture medium was supplemented with either of the following:

1. Infected/normal RBCs to a haematocrit of 5%: Blood was collected from uninfected, and 17XL (parasitemia >30%)-infected mice in ACD and washed with DMEM. Four milliliter diluted blood was layered upon 2 mL of Histopaque (Sigma-Aldrich) and spun at 1500 rpm for 20 min at RT (without brakes). RBCs were separated from PBMCs and resuspended in DMEM.
2. Crude parasite protein extract or normal RBC extract (1 mg/mL): Parasite protein extract was prepared by resuspending the parasite (*P. yoelii* 17XL) pellet in 2–3 volumes of 0.15% saponin (in PBS) containing a cocktail of protease inhibitors (1 µg/mL leupeptin, 1 µg/mL pepstatin and 0.5 mM PMSF; Sigma-Aldrich), incubated at 37°C for 15 min with intermittent mixing and centrifuged at 13 000 rpm for 10 min. The pellet was washed till the red coloration of haemoglobin was lost, resuspended in 3–4 volumes of 1% Triton X-100 (in PBS) containing the cocktail of protease inhibitors, incubated on ice for 1 h and spun at 13 000 rpm for 30 min to obtain the supernatant containing the parasite protein extract.
3. 10% Ig-depleted or undepleted serum from infected/uninfected mice: Prior to use in culture, serum was Ig-depleted using protein G-sepharose beads (GE Healthcare Life Sciences) as per manufacturer's instruction. Ig depletion was confirmed by dot-blot that was developed using the ECL Plus™ (Amersham Biosciences, Piscataway, NJ, USA).
4. 10% serum from infected mice depleted or not of IFN-γ/TNF-α: Serum from infected mice was incubated with up to 50 ng/mL of neutralizing antibody – anti-mouse IFN-γ (BD pharmingen) or anti-mouse TNF-α (BioLegend Inc) – for 6–12 h at 37°C, treated with protein G-sepharose beads to remove Ig and centrifuged at 4000 rpm before use.

Statistical analysis

Statistical significance was calculated using nonparametric Kruskal–Wallis test followed by Dunn's *post hoc* test

(GRAPHPAD INSTAT 3.0 software, La Jolla, CA, USA). The data are represented as mean \pm standard error mean (SEM). *P* values less than 0.05 were considered significant.

RESULTS

Parasite growth kinetics

Mice were infected with 10^4 infected RBCs, and parasitemia was monitored at different time points post-infection (p.i.). The 17XL infection showed rapid growth kinetics and reached a high parasitemia – $53.93 \pm 18.86\%$ ($n = 3$ mice per time point), resulting in death between Day 9 and Day 11 (Figure 1a inset). Hence, for all the experiments with the lethal strain, the mice were sacrificed at Day 8 or 9. In agreement with previous reports, 17XNL infection showed slower growth kinetics as compared to 17XL strain (11) and it resulted in a peak parasitemia of $5.52 \pm 1.41\%$ ($n = 3$ mice per time point) (Figure 1b inset). The infection was self-limiting, and the parasites were usually cleared by days 22–25.

Malarial infection causes reduction in thymic T-cell numbers

Changes in thymic weight and cell yield during both 17XL and 17XNL malarial infections were recorded at different days p.i. (Figure 1a and b). Both infections caused thymic atrophy and resulted in decreased thymic weight and thymic cellularity. Typically, the reduction in thymic weight and cellularity began later (days 5–7) in 17XL infection when the parasite load was high (parasitemia between 8 and 16%; $n = 3$) (Figure 1a). Such thymic changes began at a comparatively lower parasite load in 17XNL infection (0.98 ± 0.04 ; $n = 3$) (Figure 1b). In majority of the animals (63%), 17XNL infection-associated thymic changes occurred at parasite load as low as $4.0 \pm 1.2\%$, suggesting that the two strains had differing effects on the thymus.

P. yoelii 17XL and 17XNL infections have differing effects on thymic T-cell subpopulation numbers

Flow cytometric analysis conducted to determine the relative frequency and absolute numbers of thymocyte subsets defined by Thy 1.2, CD4, and CD8 staining revealed clear changes in the composition of the subsets following malarial infection. Thy 1.2 is one of the earliest markers on developing T cells, and numbers of DN, DP, and SP T cells were ascertained from Thy1.2⁺-gated population (Figure S1). Figure 1 shows representative dot plots of the thymus of single animals sacrificed at various time points after 17XL (c) and 17XNL (d) infection, respectively. Bar

graphs in panels (e) and (f) summarize the data of three animals from a representative experiment. The insets in panels (a) and (b) show parasitemia profiles for that particular experiment. In agreement with published data, the number of DP cells decreased in the lethal infection (5,7). The reduction in thymic weight and yield coincided with the DP decline. By Day 9, the number of DP cells in the thymus declined by ~99% of the control population (Figure 1e). Interestingly, CD4⁺ SP T-cell numbers also decreased significantly by Day 9, but this effect was less drastic (Figure 1e); the number of CD4⁺ SP T cells declined by ~87% of the control population. The numbers of DN and CD8⁺ SP T cells, on the other hand, remained unaffected.

In case of 17XNL infection, DN, DP, and CD4⁺ SP T-cell numbers were significantly affected, while CD8⁺ SP T-cell numbers remained unaffected (Figure 1f). DP T-cell numbers showed the greatest decline (>90% reduction at peak parasitemia; Figure 1f). All subpopulations started to rebound during the descending phase of the parasitemia and returned to near normal values post-parasite clearance.

Thus, 17XL and 17XNL infections resulted in thymic atrophy. Both infections resulted in decreased DP and CD4⁺ SP T-cell numbers, but only 17XNL infection led to a decrease in DN T-cell numbers as well.

Cortical but not medullary thymocytes decrease in numbers during both 17XL and 17XNL infections

Different compartments of the thymus are populated by different subpopulations of maturing thymocytes. DN cells that enter the thymus are largely found at the cortico-medullary junction and the capsule. DP cells are found in the cortex, whereas SP cells localize primarily to the medulla (25). We examined thymic sections of mice infected with the 17XL (Day 9) and 17XNL (peak parasitemia) strains to assess the effect of the infections on thymic histopathology. Histological analysis revealed a decreased cortex cellularity during late stage of 17XL (Figure 2b) and at peak parasitemia in case of 17XNL (Figure 2c) infection, but the thymic medulla remained unaffected. This selective depletion of cortical, but not medullary, thymocytes has also been observed for *P. berghei* ANKA-infected CBA mice (6). However, we did not observe a loss of delimitation of the cortico-medullary junction as reported by Andrade *et al.* (7) for *P. berghei* ANKA-infected BALB/c thymi, suggesting that the extent of histological changes in the thymus could vary depending on the species of the parasite. The dramatic reduction in DP cell numbers observed at the late stage of 17XL infection (Figure 1e) or at peak parasitemia of 17XNL infection (Figure 1f) is likely to be a major contributor to the decreased cellularity of the cortex.

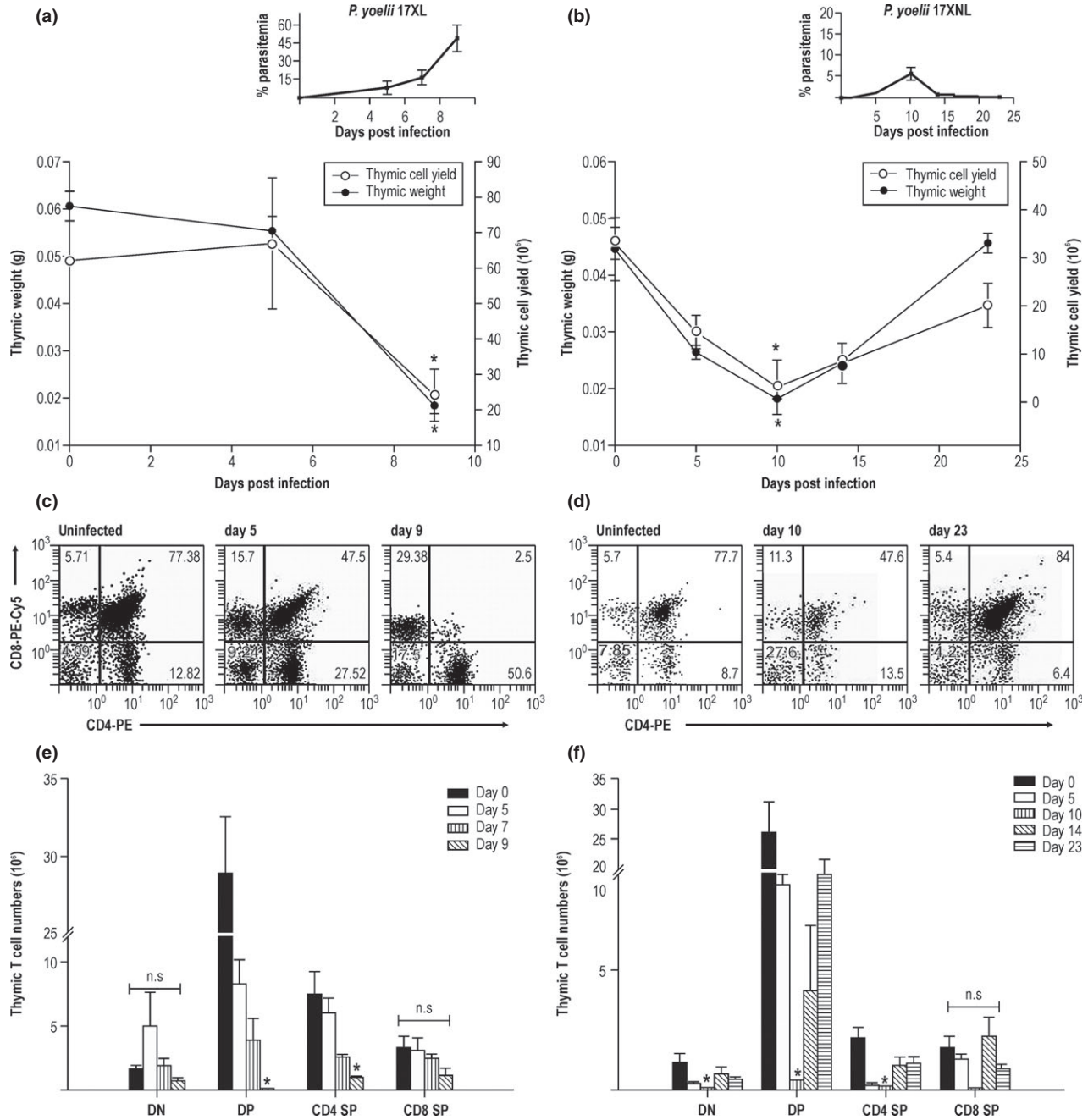


Figure 1 Change in thymic weight and T-cell numbers during *P. yoelii* 17XL (lethal) and *P. yoelii* 17XNL (nonlethal) infection in BALB/c mice. Representative graphs depicting changes in thymic weight and cell yield during lethal (a) and nonlethal (b) infection. Thymocytes from uninfected and infected mice at different days p.i. were stained with anti-Thy1.2-FITC, anti-CD4-PE and anti-CD8-PE-Cy5.5 antibodies. Representative flow cytometric dot plots of cells gated for Thy1.2⁺ cells show CD4 and CD8 SP and DP numbers at different days p.i. during lethal (c) and nonlethal (d) infection. The bar graphs (e, f) show numbers of different thymic T-cell subpopulations at different days p.i. in lethal and nonlethal infection, respectively. The insets depict the parasitemia profile of the particular experiment. Data are expressed as mean \pm SEM ($n = 3$). Similar results were obtained in three independent experiments. Statistical significance determined by Kruskal–Wallis test followed by Dunn’s *post hoc* test. * $P < 0.05$ when compared to Day 0; n.s. = not significant.

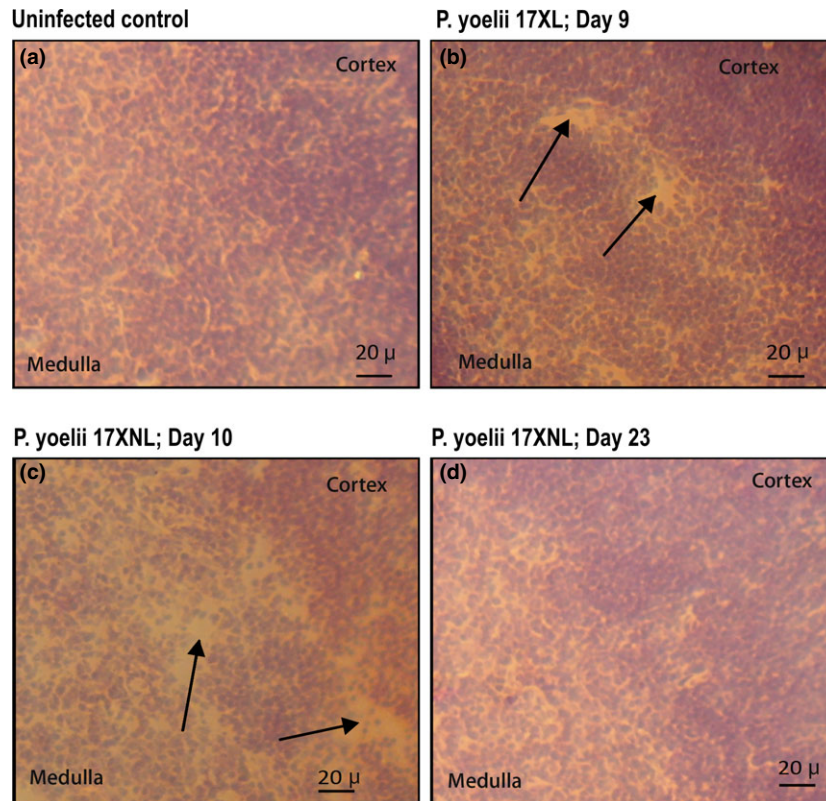


Figure 2 Depletion of cortical thymocytes during lethal and nonlethal infection. Thymic sections from uninfected (panel a) and *P. yoelii*-infected BALB/c mice (panels b–d) were stained with haematoxylin and eosin and observed at 20× magnification. *P. yoelii* 17XL-infected BALB/c mice (parasitemia = $36.9 \pm 5.3\%$) show depletion of thymocytes (arrows) from the cortex, whereas the medulla remains unaffected (b). A decrease in cortical thymocytes (arrows) was also observed at peak parasitemia in *P. yoelii* 17XNL-infected BALB/c mice (c) and the normal structure was regained post-parasite clearance (d).

Malarial infection affects surface CD8 expression on thymic T cells

Flow cytometric analysis of Thy 1.2⁺ CD4⁺ or CD8⁺ cells revealed that malarial infection resulted in a significant change in the overall surface expression of CD8 on thymic T cells, which includes cells at all stages of development. Figure 3a and b are representative histograms of Thy 1.2-gated CD8⁺ cells at Day 0 and Day 9 in 17XL infection. Figure 3c is a bar graph depicting the median fluorescence intensity (MFI) of CD4 and CD8 as the infection progresses towards lethality. The MFI for CD8 expression on developing thymocytes decreased significantly at Day 9 of 17XL infection (Figure 3c). Although CD4 showed a trend towards increased expression during the course of infection, it was not statistically significant.

The changes in surface expression of CD4 and CD8 in the course of 17XNL infection are presented in Figure 3d–h. The representative histograms in Figure 3d–g depict MFI of Thy 1.2-gated CD8⁺ cells at days 0, 5, 10, and 23 post-infection. In contrast to what was observed in

17XL infection, no significant change in surface CD8 expression was observed in the course of 17XNL infection. We observed a transient spike in CD8 expression at Day 5 post-infection (Figure 3e,h); however, it was not statistically significant ($P = 0.0704$).

Lethal and nonlethal malarial infections have differing effects on proliferation and death of thymic T-cell subpopulations

The reduced thymic cell yield could be a result of decreased rate of thymocyte proliferation or an increased thymocyte apoptosis or both. We used pulse 5-bromodeoxyuridine (BrdU) incorporation to investigate thymocyte proliferation in uninfected and 17XL- or 17XNL-infected mice. The mice were injected i.p. with 1 mg BrdU 2 h prior to sacrificing. BrdU incorporation was assessed by flow cytometric analysis of CD4⁺, CD8⁺, and BrdU⁺ cells. To examine whether apoptosis plays a role in reduction in thymic T-cell numbers during malarial infection, we performed Annexin V, CD4, and CD8 staining.

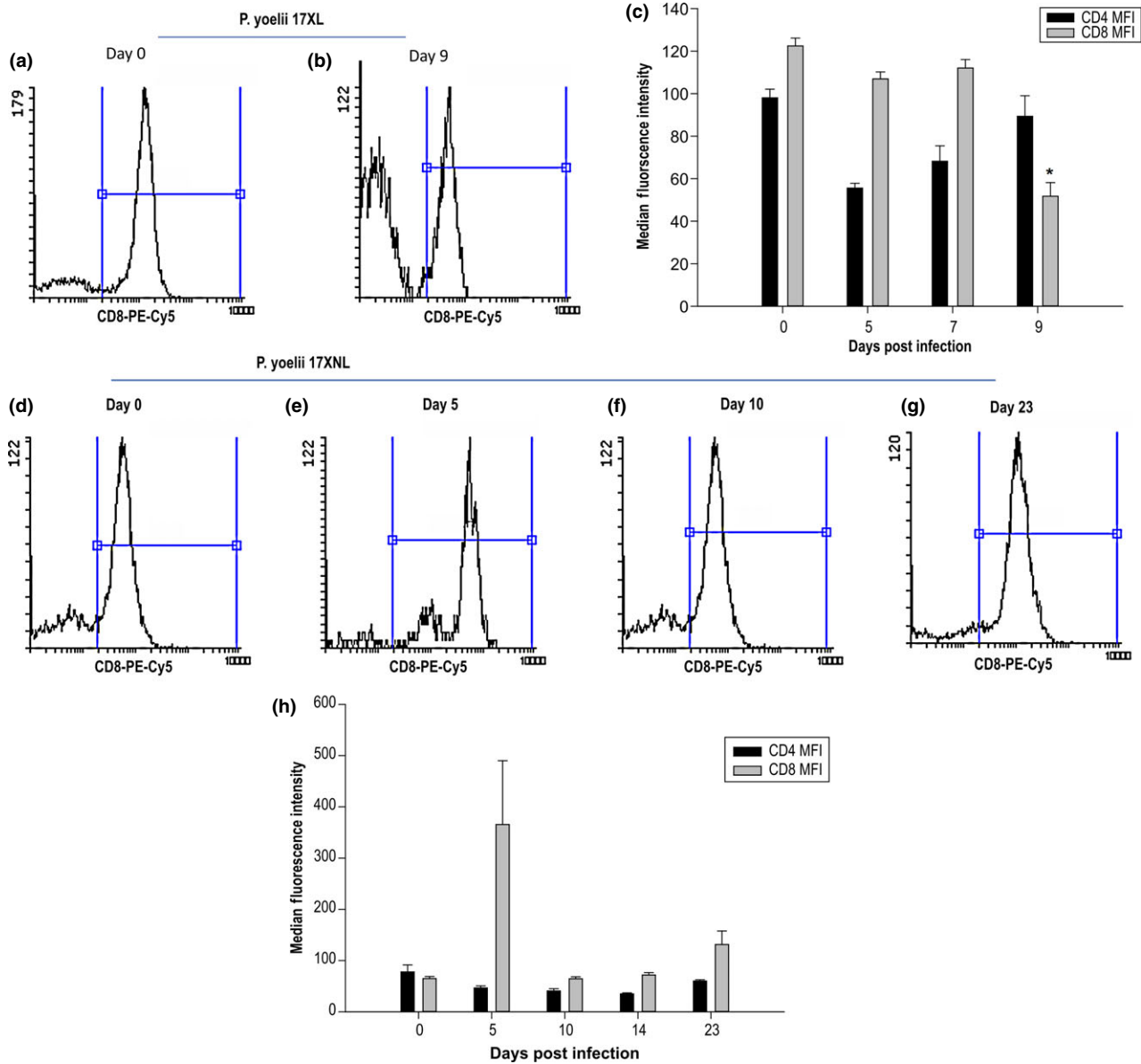


Figure 3 Alteration in surface CD8 expression on thymic T cells during *P. yoelii* 17XL (lethal) and *P. yoelii* 17XNL (nonlethal) infection in BALB/c mice. Representative histograms of CD8 expression at Day 0 (a) and Day 9 (b) on Thy1.2-gated cells in *P. yoelii* 17XL infection. (c) Bar graph showing median fluorescence intensity of CD4 and CD8 expression during the course of 17XL infection. Similarly, panels (d–g) are representative histograms showing CD8 expression on Thy1.2-gated cells at Day 0 (d), 5 (e), 10 (f) and 23 (g) during 17XNL infection. (h) Bar graph depicting median fluorescence intensity of CD4 and CD8 expression. Data are represented as mean ± SEM ($n = 3$). Statistical significance determined by Kruskal–Wallis test followed by Dunn’s *post hoc* test. * $P < 0.05$ when compared to Day 0.

Although no significant reduction in %BrdU cells was observed during the course of 17XL infection (Figure 4a), a marked reduction in %BrdU cells was observed at Day 3 post-infection (parasitemia = 1.23 ± 0.60) in 17XNL infection (Figure 4b), before peak parasitemia. This reduction in proliferation was reversible as normal level of proliferation was regained at Day 16 post-infection. Both

17XL and 17XNL infections resulted in an increase in % AnnV⁺ cells, at Day 8 post-infection in the case of former and at peak parasitemia in the latter (Figure 4c,d).

Both the reduction in proliferation and increase in apoptosis were confined to only DP T cells in 17XL infection (Figure 4e–g). In 17XNL infection, a transient reduction in proliferation of both DN and DP T cells was

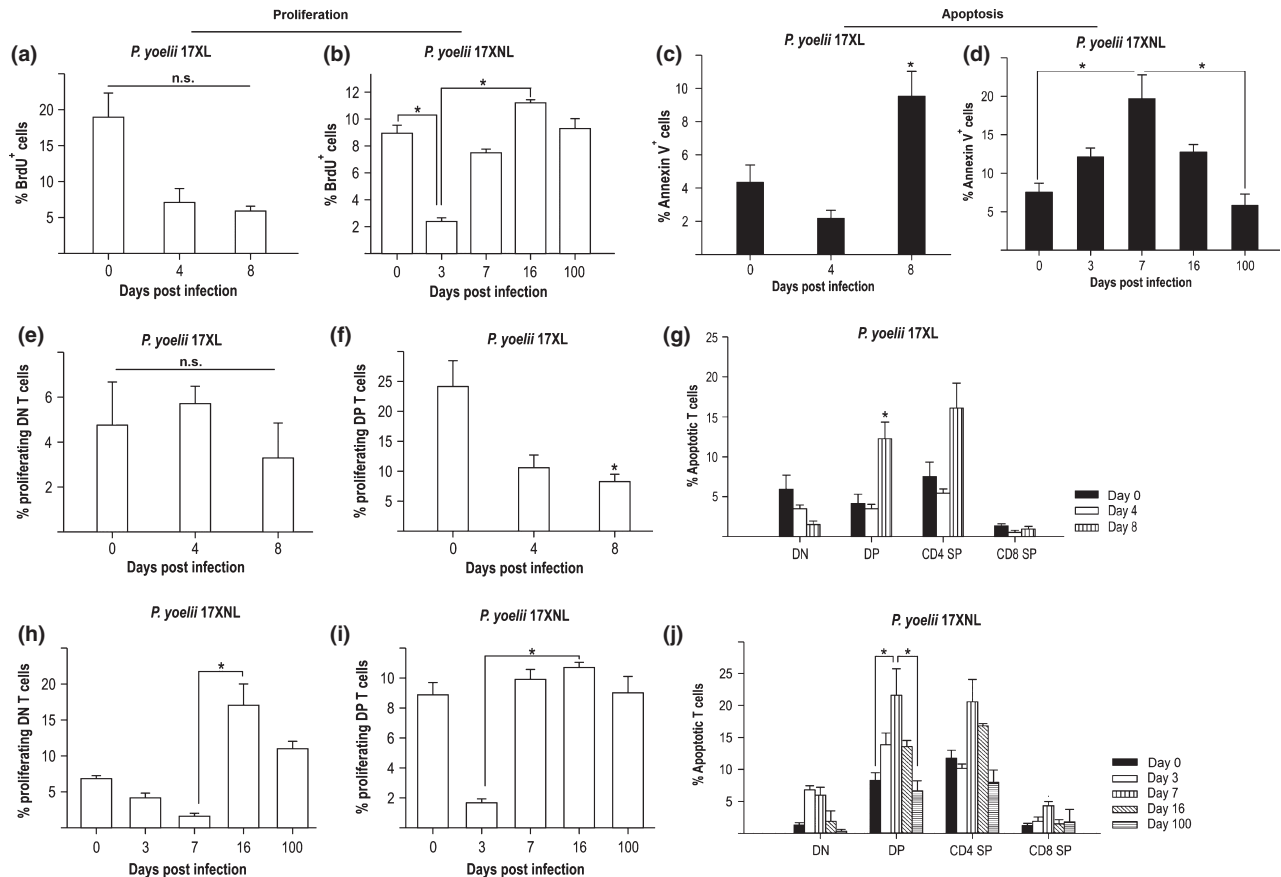


Figure 4 Decreased thymic T-cell proliferation and increased thymocyte apoptosis during infections induced by *P. yoelii* 17XL and *P. yoelii* 17XNL in BALB/c mice. Thymic cell proliferation was estimated by pulse BrdU incorporation, whereas apoptosis was determined by Annexin V staining. 17XL (panels a, e, f)- and 17XNL (panels b, h, i)-infected mice were injected i.p. with 1 mg of BrdU 2 h prior to sacrificing. Thymocytes were harvested, stained for surface CD4, CD8, fixed, permeabilized and treated with DNase I prior to staining with anti-BrdU antibodies. A decrease in total thymic T-cell proliferation (% BrdU⁺ cells; panel a) and DP T-cell proliferation (f) was observed in the lethal infection. DN T-cell proliferation remained unaltered (e). A decrease in the proliferation of total thymic (b), DN (h) and DP T cells (i) was observed during early stages of the nonlethal infection, which reverted to normal in the later stages of infection. Thymocytes from mice infected with 17XL (c, g) and 17XNL (d, j) were stained with Annexin V-FITC, anti-CD4-PE and anti-CD8-PE-Cy5 antibodies and analysed by flow cytometry. Lethal malarial infection led to an increase in total %Annexin V⁺ cells (c) and DP T cells (g). An increase in total %Annexin V⁺ cells (d) was also observed during the ascending phase of nonlethal infection with maximum apoptosis at peak parasitemia. This increase in apoptosis occurred in all the thymic subpopulations (j). The numbers of apoptosing cells reverted to normal values in the descending phase of the infection (d, j). Data are represented as mean \pm SEM ($n = 3$). Statistical significance determined by Kruskal–Wallis test followed by Dunn's *post hoc* test. * $P < 0.05$ when compared to Day 0 unless otherwise indicated. n.s. = not significant.

observed at Day 3 and Day 7 post-infection followed by a significant increase to regain the normal level of proliferation (Figure 4h–i). Such hyperplasia has been reported in a number of conditions that induce transient but reversible thymic atrophy (26). A similar increase in apoptosis in DP T cells was observed around peak parasitemia in 17XNL infection (Figure 4j).

Thus, 17XL and 17XNL infections affect DN and DP T-cell proliferation differently. The former results in reduced proliferation of DP T cells only, whereas the latter affects proliferation of both DN and DP T cells. To our

knowledge, this is the first report that demonstrates differential effects of an infection on DN and DP thymic T-cell proliferation.

Infected serum causes a reduction in DP T-cell numbers, but this effect is not attributable to either antiparasite Igs, TNF- α , or IFN- γ

We attempted to identify factor(s) responsible for increased thymic cell death and decreased cellular proliferation using *in vitro* adult thymic organ culture

(ATOC). Thymic explants from uninfected BALB/c mice were cultured under various conditions for up to 48 h and the cells were harvested and analysed by flow cytometry. When cultured in the presence of parasitized RBCs or crude parasite protein extract (*P. yoelii* 17XL), the viability and numbers of the different thymic T-cell subpopulations in the thymic explants remained unchanged (Figure S2). Serum from 17XL-infected mice was Ig-depleted using protein G-sepharose beads, and depletion was confirmed by a dot-blot (Figure 5a). Explants cultured with or without Ig-depleted serum from 17XL-infected mice (parasitemia >30%) resulted in decreased thymocyte viability and increased DP T-cell death (Figure 5b and c). This suggested that a soluble factor present in infected serum could be responsible for some of the observed effects on the thymus and that the decline in viability was not attributable to antiparasite Igs.

To determine whether serum TNF- α or IFN- γ had a role in the observed thymocyte depletion, each of these

cytokines was depleted from 17XL-infected serum using neutralizing antibodies and the cytokine-depleted sera were used in ATOC. Neutralization of either of these cytokines did not reverse the increased DP T-cell death caused by the infected serum (Figure 5d). Although DP T-cell numbers showed a downward trend when cultured in the presence of IFN- γ -depleted infected serum, this change was statistically insignificant. Further experiments will help elucidate whether IFN- γ depletion reversed the effect of malarial infection on the thymus. To summarize, the increase in DP T-cell death could not be attributed to parasite proteins, antiparasite Igs, IFN- γ , or TNF- α .

DISCUSSION

Severe reversible atrophy of the thymus has been reported during acute sepsis, viral, bacterial, fungal, and protozoan diseases (27). However, systematic studies establishing the effect of these infections on the thymus and the developing thymocyte subpopulations have received less attention. In

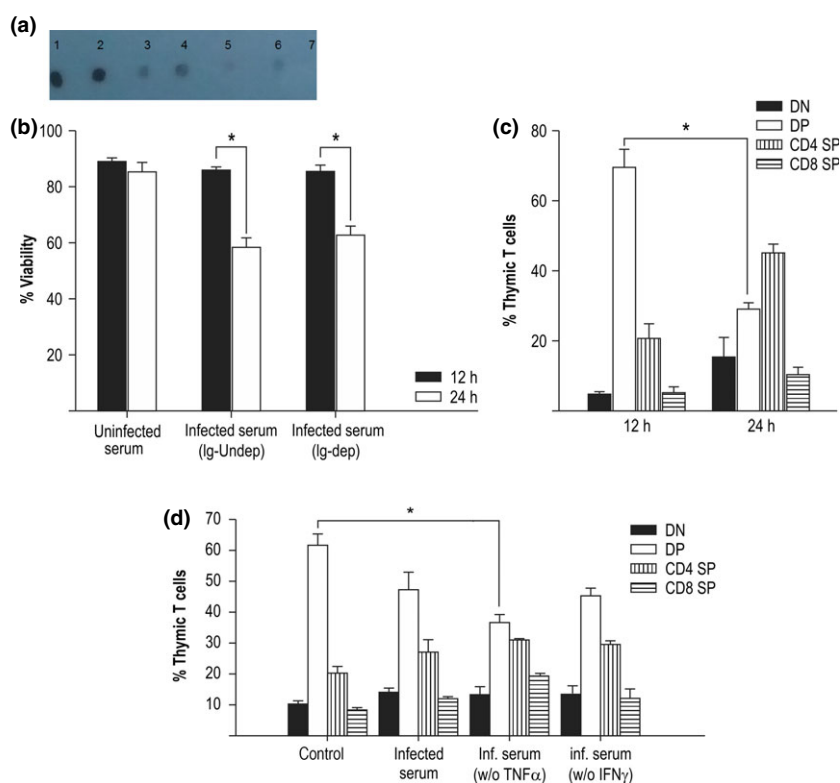


Figure 5 Serum-derived factors other than the cytokines TNF- α and IFN- γ cause decrease in thymocyte viability and DP T cells. Serum was depleted of Ig using protein G-sepharose beads (a). The viability and proportions of different thymic T-cell subpopulations of thymic explants cultured in the presence of Ig-depleted (b,c) and Ig-undepleted (b) infected serum was estimated at 12 and 24 h time points (b,c). Panel (b) depicts % viability of the thymocytes at 12 and 24 h. Panel (c) shows the percentage of DN, DP and SP cells at different time points in the explants. Panel (d) depicts the changes in viability of different subsets in the explants cultured in the presence of serum depleted of TNF- α or IFN- γ . Data are represented as mean \pm SEM ($n = 3$). Statistical significance determined by Kruskal–Wallis test followed by Dunn's *post hoc* test. * $P < 0.05$.

this study, we have investigated the effects of *P. yoelii* 17XL and 17XNL infections on the thymic T-cell subsets in BALB/c mice. We found that both strains differentially affect thymocyte death and proliferation. In addition, they also affect CD8 expression on the developing thymocytes.

In agreement with earlier reports, we found that both 17XL and 17XNL malarial infections resulted in thymic involution and reduced cell yield (5–7). The effects of 17XL infection were evident predominantly in the later stages of the infection when parasitemia exceeded 10%, whereas the effect of 17XNL infection was observed at very early stages of the infection, when the parasitemia was $0.98 \pm 0.04\%$, suggesting that these effects were neither directly related to parasite load nor were they a function of the number of days the mice were exposed to the parasite.

The earliest observed effect on the thymus, in both lethal and nonlethal infection, was the disappearance of DP T cells with concomitant thymic atrophy. This atrophy was attributable to increased thymocyte apoptosis and decreased thymocyte proliferation. The thymocyte subpopulations were differentially affected by the two strains of the parasite used. 17XL infection predominantly affected only DP and CD4⁺ SP T cells. However, all the developing subpopulations except CD8⁺ T cells underwent drastic reduction in numbers early during the ascending phase of 17XNL infection.

In a healthy young adult, DP T cells form ~80% of the developing T-cell population in the thymus and this subset is central to the T-cell developmental process (28–30). During the DP-to-SP stage transition, the cells are subjected to selective pressure and only ~5% cells survive the selection processes. Our data show > 80% reduction in DP numbers during both 17XL and 17XNL infection. This reduction was the result of increased apoptosis and decreased proliferation. Typically, almost 95% of the developing thymocytes undergo apoptosis in the thymus as they fail to express TcRs with an optimal affinity for the selecting intrathymic peptide–MHC complexes (20,31,32). Majority of the cells undergoing apoptosis are at the DP stage of development, and DP cells are known to be apoptosis-sensitive (21,33). Hence, it was not surprising that both the infections resulted in apoptosis of DP T cells, as has been reported for other murine malarial infections (5,7). In the course of their ontogeny, developing thymocytes undergo massive proliferation before TcR gene rearrangement. This proliferation occurs at two distinct stages of development. The first expansion occurs during DN1-to-DN3 transition before the TCR β gene rearrangement, and the second occurs during the DN–DP transition before TCR α gene rearrangement (34,35). The control of these proliferative stages and the molecular players

involved are still being investigated, although signalling through MYC, NOTCH1 and IL7R is known to be involved (36). We found that 17XL and 17XNL infections affected proliferation of developing T cells differently. Only DP stage proliferation was reduced in 17XL infection, whereas proliferation of both DN and DP stages was affected in 17XNL infection. Further investigations are needed to understand the mechanism underlying this effect.

Another major finding was that 17XL infection resulted in a decrease in surface CD8 expression in developing thymocytes with increasing parasitemia. In 17XNL infection, there was a transient upward trend in surface CD8 expression in the early stages of infection; however, this increase was not statistically significant. Such changes in thymic coreceptor expression have not been reported in any other infection (27). Recent transcriptome analysis suggests that apart from the *Cd4*, *Cd8a*, *Cd8b1* and *Rorc* genes, several regulators such as *Chd1*, *Klf7*, *Mef2a*, *Meir1*, *Pou6f1* and *Suhw4* (*Zfp280d*) maybe involved in transition from DN to immature single-positive stage when CD8 is first expressed on the thymocytes (36). However, regulators involved in controlling levels of CD8 expression in the developing thymocytes remain unknown. Changes in surface CD8 expression on developing thymocytes are likely to affect the thymocyte selection. T-cell maturation involves positive and negative selection, both of which are mediated by interactions between a TCR and CD4 or CD8 on a maturing thymocyte and an MHC–self-peptide ligand on a selecting cell. Studies have shown that thymocytes expressing markedly enhanced levels of CD8 are selectively deleted in the process of thymic maturation (37–40). Thus, it is likely that the aberrant transient increase in surface CD8 expression in the early stages of the 17XNL infection and the decline in the later stages of infection could affect the process of T-cell maturation.

Adult thymic organ culture is an accessible means to study thymic T-cell maturation while maintaining the thymic microenvironmental architecture and the three-dimensional cellular interactions. It has been used in the past to identify factors that may play a role in thymocyte apoptosis and proliferation (41,42). In this study, ATOC was undertaken in an attempt to understand the molecular players responsible for the observed thymic atrophy. No change in thymocyte viability was observed when thymic explants were cultured in the presence of infected RBCs and parasite protein extract, suggesting that parasite proteins may not have a direct effect on thymocyte viability. However, explants cultured in medium supplemented with serum from infected mice showed decrease in DP T-cell numbers. Malarial infection results in increased serum levels of IFN- γ and TNF- α (12,43–46). Both these cyto-

kines have been shown to be involved in DP T-cell death (47–51). In this study, neutralization of TNF- α and IFN- γ did not alter the apoptosis-inducing capacity of the serum. In fact, TNF- α neutralization resulted in a further reduction in DP T-cell numbers. This could mean that in malaria-induced thymic atrophy, TNF- α plays a protective rather than a destructive role. This is contrary to what is observed in Chagas' disease, another parasitic infection caused by a closely related apicomplexan *Trypanosoma cruzi*, where severe thymocyte depletion has been observed in parallel with increased TNF- α levels. However, this depletion is attributed to TNF-induced glucocorticoids rather than TNF- α directly (51). Thus, it is likely that it is not the cytokines *per se*, but downstream molecules induced by them that are responsible for some of the observed thymic changes.

The immunopathogenesis of murine malarial infection varies with the combination of *Plasmodium* species and rodent host. Here, we used two different strains of *P. yoelii*, 17XL (lethal) and 17XNL (nonlethal), to infect the same rodent host, BALB/c mice, and observed the effects induced by both parasite strains on the thymus. The effects induced by the nonlethal strain were reversible, with the thymic T-cell numbers, apoptosis and proliferation, all returning back to normal levels in the descending phase of parasitemia. The recovery of mice from infection is unlikely to be due to the addition of recent thymic emigrants to the peripheral naïve T-cell pool during the course of infection. Typically, the process of T-cell maturation takes around 12–15 days, with the DN to DP differentiation occurring in the first 7 days (17). In this study, we observed the malarial parasite-induced thymic effects (and recovery in the case of nonlethal infection) within a much shorter time span; therefore, recent thymic emigrants may not be involved in the immune response leading to parasite clearance. Instead, these effects could be attributed to distinct immunomodulatory functions employed by these two parasite strains (2). Dendritic cells isolated from mice with *P. yoelii* 17XNL infection have been shown to be fully functional, leading to stimulation of T-cell proliferation, IL-12 secretion, effective immunoregulatory responses involving IL-10, TGF- β , and IL-27 (52). Furthermore, Fu *et al.* (53) have shown that macrophage-mediated innate response in case of *P. yoelii* 17XNL plays a critical role in early control of parasitemia, a when compared to *P. yoelii* 17XL and is attributed to the upregulation of the expression of TLR2 and intracellular signalling molecules MyD88, IRAK-1 and TRAF-6. The presence of these differential immunoregulatory mechanisms in lethal and nonlethal strains may explain why despite severe effects on the thymic T-cell popula-

tions around peak parasitemia, mice infected with nonlethal strain manage to recover from the infection and regain normal thymic T-cell numbers, apoptosis and proliferation levels.

In conclusion, this study investigating the effect of two closely related malarial parasite strains on the murine thymus reveals that although both infections cause thymic atrophy, there is substantial difference in the manner in which they affect the thymus. The lethal strain (17XL) causes reduction in numbers of DP and CD4⁺ SP T cells, affects proliferation of DP T cells and downregulates CD8 expression on the thymic T-cell subpopulations. The nonlethal strain (17XNL) induces reversible but more profound effects at much lower parasitemia. It causes early and rapid death of DN, DP, and CD4⁺ T-cell subpopulations and affects the proliferation of DN and DP T cells. ATOC showed that the increase in DP T-cell death could not be attributed to parasite proteins, antiparasite Igs, IFN- γ or TNF- α .

A better understanding of the mechanisms that cause these thymic changes during malarial infection, especially those leading to the reversible involution of the thymus in case of nonlethal infection, would add to the current information regarding host–parasite interactions. Although detailed studies on the effect of the malarial infections on human thymus are lacking, a recent report links a decrease in thymus size to malaria (54). Whether malaria-induced thymic atrophy and its interference with T-cell development affect the number and/or repertoire of naïve T cells egressing to the periphery remains unclear. This and other murine studies suggest that the thymic changes may not be relevant to the outcome of a single round of infection (5–7). However, investigations are clearly needed to assess the impact of chronic malarial infection on the naïve T-cell repertoire of individuals, especially children and young adults, living in hyperendemic malarial regions.

ACKNOWLEDGEMENTS

The authors thank Dr. S. Chiplunkar for her critical inputs. We are grateful to Dr. M. Mehta and Dr. B.A. Mannan for critical reading of the manuscript. This work was supported by an intramural grant from TIFR and from Department of Science and Technology, India.

AUTHOR CONTRIBUTIONS

SS and SP conceived the experiments. SK and SP performed the experiments. All the authors were involved in the writing of the manuscript.

REFERENCES

- 1 Sanni LA, Fonseca LF & Langhorne J. Mouse models for erythrocytic-stage malaria. *Methods Mol Med* 2002; **72**: 57–76.
- 2 Wykes MN & Good MF. What have we learnt from mouse models for the study of malaria? *Eur J Immunol* 2009; **39**: 2004–2007.
- 3 Schofield L & Grau GE. Immunological processes in malaria pathogenesis. *Nat Rev Immunol* 2005; **5**: 722–735.
- 4 Good MF, Xu H, Wykes M, et al. Development and regulation of cell-mediated immune responses to the blood stages of malaria: implications for vaccine research. *Annu Rev Immunol* 2005; **23**: 69–99.
- 5 Seixas E & Ostler D. *Plasmodium chabaudi chabaudi* (AS): differential cellular responses to infection in resistant and susceptible mice. *Exp Parasitol* 2005; **110**: 394–405.
- 6 Carvalho LJM, Ferreira-da-cruz MF, Daniel-Ribeiro CT, et al. *Plasmodium berghei* ANKA infection induces thymocyte apoptosis and thymocyte depletion in CBA mice. *Mem Inst Oswaldo Cruz* 2006; **101**: 523–528.
- 7 Andrade CF, Gameiro J, Nagib PRA, et al. Thymic alterations in *Plasmodium berghei*-infected mice. *Cell Immunol* 2008; **253**: 1–4.
- 8 Pattaradilokrat S, Cheesman SJ & Carter R. Congenicity and genetic polymorphism in cloned lines derived from a single isolate of a rodent malaria parasite. *Mol Biochem Parasitol* 2008; **157**: 244–247.
- 9 Otsuki H, Kaneko O, Thongkukiatkul A, et al. Single amino acid substitution in *Plasmodium yoelii* erythrocyte ligand determines its localization and controls parasite virulence. *Proc Natl Acad Sci USA* 2009; **106**: 7167–7172.
- 10 Culleton R & Kaneko O. Erythrocyte binding ligands in malaria parasites: intracellular trafficking and parasite virulence. *Acta Trop* 2010; **114**: 131–137.
- 11 Martin-Jaular L, Ferrer M, Calvo M, et al. Strain-specific spleen remodelling in *Plasmodium yoelii* infections in Balb/c mice facilitates adherence and spleen macrophage-clearance escape. *Cell Microbiol* 2011; **13**: 109–122.
- 12 Choudhury HR, Sheikh NA, Bancroft GJ, et al. Early nonspecific immune responses and immunity to blood-stage nonlethal *Plasmodium yoelii* malaria. *Infect Immun* 2000; **68**: 6127–6132.
- 13 Omer FM, de Souza JB & Riley EM. Differential induction of TGF-beta regulates pro-inflammatory cytokine production and determines the outcome of lethal and nonlethal *Plasmodium yoelii* infections. *J Immunol* 2003; **171**: 5430–5436.
- 14 Weiss L, Geduldig U & Weidanz W. Mechanisms of splenic control of murine malaria: reticular cell activation and the development of a blood-spleen barrier. *Am J Anat* 1986; **176**: 251–285.
- 15 Drumea-Mirancea M, Wessels JT, Müller CA, et al. Characterization of a conduit system containing laminin-5 in the human thymus: a potential transport system for small molecules. *J Cell Sci* 2006; **119**: 1396–1405.
- 16 Schwarz BA, Sambandam A, Maillard I, et al. Selective thymus settling regulated by cytokine and chemokine receptors. *J Immunol* 2007; **178**: 2008–2017.
- 17 Vasseur F, Le Campion A & Pénit C. Scheduled kinetics of cell proliferation and phenotypic changes during immature thymocyte generation. *Eur J Immunol* 2001; **31**: 3038–3047.
- 18 Miyazaki M, Miyazaki K, Itoi M, et al. Thymocyte proliferation induced by pre-T cell receptor signaling is maintained through polycomb gene product Bmi-1-mediated Cdkn2a repression. *Immunity* 2008; **28**: 231–245.
- 19 Huesmann M, Scott B, Kisielow P, et al. Kinetics and efficacy of positive selection in the thymus of normal and T cell receptor transgenic mice. *Cell* 1991; **66**: 533–540.
- 20 Starr TK, Jameson SC & Hogquist KA. Positive and negative selection of T cells. *Annu Rev Immunol* 2003; **21**: 139–176.
- 21 Jiang D, Zheng L & Lenardo MJ. Caspases in T-cell receptor-induced thymocyte apoptosis. *Cell Death Differ* 1999; **6**: 402–411.
- 22 Lucas B, Vasseur F & Penit C. Normal sequence of phenotypic transitions in one cohort of 5-bromo-2'-deoxyuridine-pulse-labeled thymocytes. Correlation with T cell receptor expression. *J Immunol* 1993; **151**: 4574–4582.
- 23 Achtman AH, Khan M, MacLennan ICM, et al. *Plasmodium chabaudi chabaudi* infection in mice induces strong B cell responses and striking but temporary changes in splenic cell distribution. *J Immunol* 2003; **171**: 317–324.
- 24 Whalen BJ, Weiser P, Marounek J, et al. Recapitulation of normal and abnormal B-cell development in adult thymus organ culture. *J Immunol* 1999; **162**: 4003–4012.
- 25 Teng F, Zhou Y, Jin R, et al. The molecular signature underlying the thymic migration and maturation of TCR $\alpha\beta$ ⁺ CD4⁺ CD8 thymocytes. *PLoS ONE* 2011; **6**: e25567.
- 26 Taub DD & Longo DL. Insights into thymic aging and regeneration. *Immunol Rev* 2005; **205**: 72–93.
- 27 Savino W. The thymus is a common target organ in infectious diseases. *PLoS Pathog* 2006; **2**: e62.
- 28 Takahama Y. Journey through the thymus: stromal guides for T-cell development and selection. *Nat Rev Immunol* 2006; **6**: 127–135.
- 29 Kappes DJ, He X & He X. CD4-CD8 lineage commitment: an inside view. *Nat Immunol* 2005; **6**: 761–766.
- 30 Gruver AL & Sempowski GD. Cytokines, leptin, and stress-induced thymic atrophy. *J Leukoc Biol* 2008; **84**: 915–923.
- 31 Aliahmad P & Kaye J. Commitment issues: linking positive selection signals and lineage diversification in the thymus. *Immunol Rev* 2006; **209**: 253–273.
- 32 Palmer E. Negative selection—clearing out the bad apples from the T-cell repertoire. *Nat Rev Immunol* 2003; **3**: 383–391.
- 33 Xue L, Chiang L, He B, et al. FoxM1, a forkhead transcription factor is a master cell cycle regulator for mouse mature T cells but not double positive thymocytes. *PLoS ONE* 2010; **5**: e9229.
- 34 Kawamoto H, Ohmura K, Fujimoto S, et al. Extensive proliferation of T cell lineage-restricted progenitors in the thymus: an essential process for clonal expression of diverse T cell receptor beta chains. *Eur J Immunol* 2003; **33**: 606–615.
- 35 Ikawa T, Masuda K, Lu M, et al. Identification of the earliest prethymic T-cell progenitors in murine fetal blood. *Blood* 2004; **103**: 530–537.
- 36 Mingueneau M, Kreslavsky T, Gray D, et al. The transcriptional landscape of $\alpha\beta$ T cell differentiation. *Nat Immunol* 2013; **14**: 619–632.
- 37 Lee NA, Loh DY & Lacy E. CD8 surface levels alter the fate of alpha/beta T cell receptor-expressing thymocytes in transgenic mice. *J Exp Med* 1992; **175**: 1013–1025.
- 38 Wack A, Coles M, Norton T, et al. Early onset of CD8 transgene expression inhibits the transition from DN3 to DP thymocytes. *J Immunol* 2000; **165**: 1236–1242.
- 39 Robey EA, Ramsdell F, Kioussis D, et al. The level of CD8 expression can determine the outcome of thymic selection. *Cell* 1992; **69**: 1089–1096.
- 40 Smith DH, Lee N & Lacy E. Thymocyte cell fate alteration by high levels of CD8alpha is independent of CD8-lck association. *J Immunol* 1996; **157**: 1087–1095.
- 41 Anderson G & Jenkinson EJ. Thymus organ cultures and T-cell receptor repertoire development. *Immunology* 2000; **100**: 405–410.
- 42 Radojević K, Rakin A, Pilipović I, et al. Effects of catecholamines on thymocyte apoptosis and proliferation depend on thymocyte microenvironment. *J Neuroimmunol* 2014; **272**: 16–28.
- 43 Artavanis-Tsakonas K & Riley EM. Innate immune response to malaria: rapid induction of IFN-gamma from human NK cells by live *Plasmodium falciparum*-infected erythrocytes. *J Immunol* 2002; **169**: 2956–2963.
- 44 Yoneto T, Yoshimoto T, Wang CR, et al. Gamma interferon production is critical for protective immunity to infection with blood-stage *Plasmodium berghei* XAT but neither NO production nor NK cell activation is critical. *Infect Immun* 1999; **67**: 2349–2356.
- 45 Grau GE, Pigué PF, Vassalli P, et al. Tumor-necrosis factor and other cytokines in cerebral malaria: experimental and clinical data. *Immunol Rev* 1989; **112**: 49–70.
- 46 Molyneux ME, Engelmann H, Taylor TE, et al. Circulating plasma receptors for tumour necrosis factor in Malawian children

- with severe falciparum malaria. *Cytokine* 1993; **5**: 604–609.
- 47 Guevara Patiño JA, Marino MW, Ivanov VN, *et al.* Sex steroids induce apoptosis of CD8+CD4+ double-positive thymocytes via TNF-alpha. *Eur J Immunol* 2000; **30**: 2586–2592.
- 48 Pérez AR, Roggero E, Nicora A, *et al.* Thymus atrophy during *Trypanosoma cruzi* infection is caused by an immuno-endocrine imbalance. *Brain Behav Immun* 2007; **21**: 890–900.
- 49 Liepinsh DJ, Kruglov AA, Galimov AR, *et al.* Accelerated thymic atrophy as a result of elevated homeostatic expression of the genes encoded by the TNF/lymphotoxin cytokine locus. *Eur J Immunol* 2009; **39**: 2906–2915.
- 50 Fayad R, Sennello JA, Kim S-H, *et al.* Induction of thymocyte apoptosis by systemic administration of concanavalin A in mice: role of TNF-alpha, IFN-gamma and glucocorticoids. *Eur J Immunol* 2005; **35**: 2304–2312.
- 51 Cohen O, Kfir-Erenfeld S, Spokoini R, *et al.* Nitric oxide cooperates with glucocorticoids in thymic epithelial cell-mediated apoptosis of double positive thymocytes. *Int Immunol* 2009; **21**: 1113–1123.
- 52 Wykes MN, Liu XQ, Beattie L, *et al.* Plasmodium strain determines dendritic cell function essential for survival from malaria. *PLoS Pathog* 2007. DOI: 10.1371/journal.ppat.0030096
- 53 Fu Y, Ding Y, Zhou T, *et al.* *Plasmodium yoelii* blood-stage primes macrophage-mediated innate immune response through modulation of toll-like receptor signaling. *Malar J* 2012; **11**: 104.
- 54 Garly M-L, Trautner SL, Marx C, *et al.* Thymus size at 6 months of age and subsequent child mortality. *J Pediatr* 2008; **153**: 683–688, 688.e1–3.

SUPPORTING INFORMATION

Additional Supporting Information may be found in the online version of this article:

Figure S1. Flow cytometry gating strategies for thymocyte subset identification.

Figure S2. Effect of iRBCs and parasite proteins on thymocyte viability of thymic explants.